**4876** *J. Phys. Chem. A* **2000,** *104,* 4876−4881

# Solvent Polarity Dependence of Photoinduced Charge Separation in a Tetrathiophene-$C_{60}$ Dyad Studied by Pico- and Nanosecond Laser Flash Photolysis in the Near-IR Region

**Mamoru Fujitsuka,**[†] **Osamu Ito,***[,†] **Takashi Yamashiro,**[‡] **Yoshio Aso,**[‡] **and Tetsuo Otsubo***[,‡]

*Institute for Chemical Reaction Science, Tohoku University, Katahira, Aoba-ku, Sendai, 980-8577, Japan and Department of Applied Chemistry, Faculty of Engineering, Hiroshima University, Higashi-hiroshima, 739-8527, Japan*

*Received: January 11, 2000; In Final Form: March 9, 2000*

Photoinduced charge separation and recombination processes in a tetrathiophene−$C_{60}$ dyad molecule (4T-$C_{60}$) in various solvents were investigated by observing transient absorption spectra in the near-IR region. In polar solvents such as tetrahydrofuran and benzonitrile, charge separation occurred at a rate on the order of $10^{10}$ $s^{-1}$, which decreased down to the order of $10^9$ $s^{-1}$ in moderately polar solvents. In nonpolar toluene, charge separation was not observed. The quantum yields for the charge separations were nearly unity in polar solvents. Charge recombination occurred in 100 ps − 10 ns; the shorter lifetimes occurred in the highly polar solvents. After recombination, the triplet excited state of $C_{60}$ was generated predominantly. In polar solvents such as benzonitrile, the charge-separated state was also observed in the microsecond time region. To explain the unprecedented long lifetime of the second charge-separation step, an equilibrium between the charge-separated state and the triplet excited state was taken into consideration.

## Introduction

Recently, fullerene ($C_{60}$) has been adopted in several donor−acceptor-linked molecules in order to realize an efficient photoinduced charge-separation process.[1−6] In such dyad molecules, fullerene acts as an electron acceptor. As for the donor of the dyad molecules, aniline,[1] carotenoid,[2] porphyrin,[2b,3,4] pyrazine,[5] and so forth[6] have been employed. In these molecules, the quantum yields of the charge-separation processes were close to unity. The lifetimes of the charge-separated states were on the order of subnanoseconds. Imahori et al. reported that the reorganization energy of the dyad molecule including the fullerene acceptor is small compared with other reported electron acceptors.[4b] This feature seems to be one of the advantages of the fullerene-containing dyad molecules, the use of which is aimed at attaining a long-lived charge-separated state with high quantum yield for application to energy-storage systems or other sensitized reactions. As for the donor moiety of the dyad molecule, several candidates are expected in addition to those listed above because many examples of photoinduced electron-transfer reactions between fullerene and donors have been reported.[7−12] Studies on various donor−fullerene dyad molecules are expected to give important information in optimizing the charge-separation yield and lifetime.

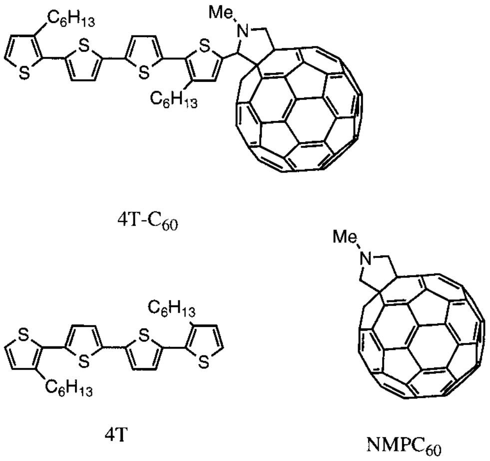

**Figure 1.** Molecular structures of 4T-$C_{60}$, NMPC$_{60}$, and 4T.

In the present study, we examined the photoinduced charge-separation and recombination processes in a novel tetrathiophene−$C_{60}$ linked dyad molecule (Figure 1) by time-resolved absorption and fluorescence measurements. Oligothiophenes have been confirmed to donate an electron to the triplet-excited fullerenes in solution in previous studies.[13,14] In the polythiophene film doped with $C_{60}$, ultrafast photoinduced charge generation was reported.[15] The present dyad molecule has a rather strict structure due to a stiff oligothiophene structure, although the alkyl chain was introduced to realize higher solubility of the dyad molecule in various organic solvents. Furthermore, oligothiophenes are stable compared with other olefins such as carotenoid because of stabilization of the $\pi$-conjugated chain by the sulfur atom. By applying pico- and nanosecond laser flash photolysis techniques to the present dyad molecule, absorption bands due to the charge-separation species were successfully observed in the near-IR region. The solvent dependence of charge-separation and recombination rates are disclosed. Furthermore, unprecedentedly long charge separation in the microsecond time region is reported.

## Experimental Section

**Materials.** Syntheses of the dihexyltetrathiophene−$C_{60}$ dyad (4T-$C_{60}$), *N*-methylpyrrolidino−$C_{60}$ (NMPC$_{60}$), and dihexyltetrathiophene (4T) were described in a previous paper (Figure 1).[16] Other chemicals were of the best commercial grade available.

---

* To whom correspondence should be addressed.

[†] Tohoku University.

[§] Hiroshima University.

10.1021/jp000136j CCC: $19.00

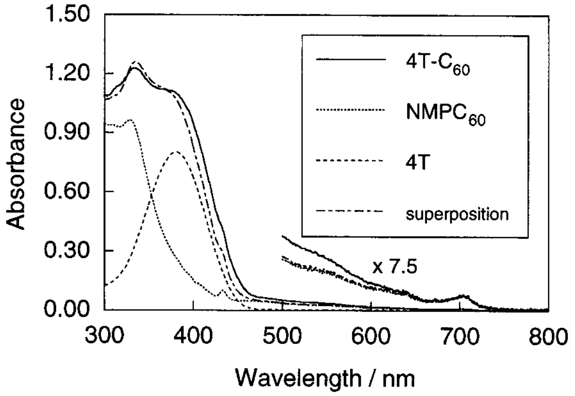

**Figure 2.** Absorption spectra of 4T-C$_{60}$, NMPC$_{60}$, and 4T in toluene. Superposition of NMPC$_{60}$ and 4T is indicated by dash-dot line.

**Apparatus.** The time-resolved fluorescence spectra were measured by a single-photon counting method using the second harmonic generation (SHG, 410 nm) of a Ti:sapphire laser (Spectra-Physics, Tsunami 3950-L2S, 1.5 ps fwhm) as an excitation source and a streakscope (Hamamatsu Photonics, C4334-01) equipped with a polychromator (Acton Research, SpectraPro 150) as a detector.

The picosecond laser flash photolysis was carried out using a SHG (532 nm) of an active/passive mode-locked Nd:YAG laser (Continuum, PY61C-10, fwhm 35 ps) as the excitation light. A white continuum pulse generated by focusing the fundamental of the Nd:YAG laser on a $D_2O/H_2O$ (1:1 volume) cell was used as the monitoring light. The visible monitoring light transmitted through the sample was detected with a Dual MOS detector (Hamamatsu Photonics, C6140) equipped with a polychromator (Acton Research, SpectraPro 150). For detection of the near-IR light, an InGaAs linear image sensor (Hamamatsu Photonics, C5890-128) was employed as the detector. The spectra were obtained by averaging 80 events on a microcomputer. The time resolution of the present system was ca. 35 ps.

Nanosecond transient absorption measurements were carried out using a SHG (532 nm) of a Nd:YAG laser (Spectra-Physics, Quanta-Ray GCR-130, fwhm 6 ns) as an excitation source. For transient absorption spectra in the near-IR region (600−1600 nm), monitoring light from a pulsed Xe lamp was detected with a Ge-avalanche photodiode (Hamamatsu Photonics, B2834). Photoinduced events in micro- and millisecond time regions were estimated by using a continuous Xe lamp (150 W) and an InGaAs−PIN photodiode (Hamamatsu Photonics, G5125-10) as a probe light and detector, respectively. Details of the transient absorption measurements were described in our previous papers.[12] All the samples in a quartz cell (1 × 1 cm) were deaerated by bubbling Ar through the solution for 15 min.

Steady-state absorption spectra in the visible and near-IR regions were measured on a Jasco V570 DS spectrophotometer.

## Results and Discussion

**Steady-State Absorption Spectra.** Figure 2 shows an absorption spectrum of 4T-C$_{60}$ in toluene as well as those of 4T and NMPC$_{60}$, which correspond to components of 4T-C$_{60}$. The absorption peaks and shoulders of 4T-C$_{60}$ were interpreted from the superposition of the components as indicated in Figure 2. A slight broadening of the absorption band of 4T-C$_{60}$ was observed in the region of 380−470 nm compared with the superposition of the components, which indicates very weak interaction among the components due to a close distance. In the present laser flash photolysis study, excitation was carried out by the 532-nm laser light, which predominantly excites the C$_{60}$ moiety of the dyad. Very weak interaction between C$_{60}$ and 4T moieties is in accord with the results of electrochemical analysis: Oxidation and reduction potentials of 4T-C$_{60}$ (1.04 and −0.63 V vs Ag/AgCl in benzonitrile, respectively) are almost the same as the oxidation potential of 4T (1.07 V) and the reduction potential of NMPC$_{60}$ (−0.63 V).[16] The rigid tetrathienyl group may exclude structural variation, which brings about a weak interaction in the ground state, although in a film mixture composed of C$_{60}$ and polythiophene or oligothiophene, substantial interaction among them was confirmed in the absorption spectra.[15]

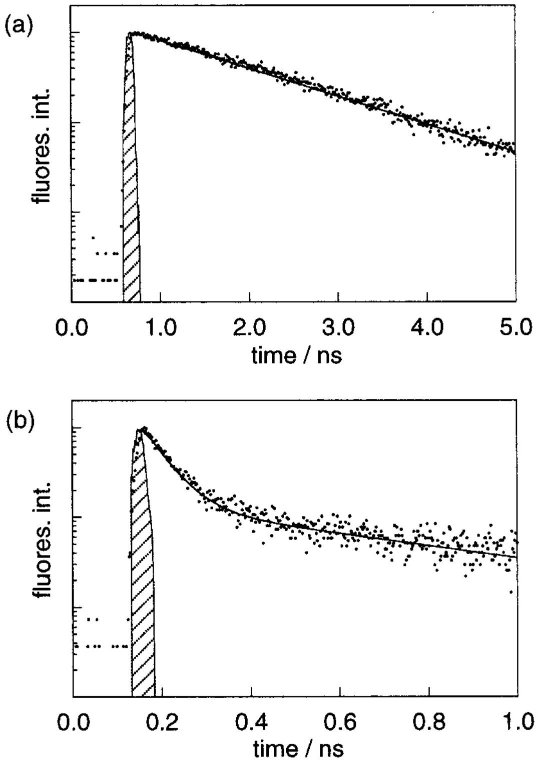

**Figure 3.** Fluorescence decay profiles around 710 nm of 4T-C$_{60}$ in (a) toluene and (b) benzonitrile. Excitation is at 410 nm. Solid lines show fitted curves; hatched parts indicate laser profile.

**Time-Resolved Fluorescence Measurement.** In a previous paper, it was reported that the fluorescence peaks of unbonded 4T at 460 and 484 nm disappeared because of the connection with C$_{60}$ in toluene.[16] Thus, the fluorescence bands due to the C$_{60}$ moiety were observed at 712 and 790 nm, which have the same lifetime as that of NMPC$_{60}$ (Figure 3a). These findings indicate that the fast energy transfer from the singlet excited state of 4T to C$_{60}$ occurs (eq 1) to generate the singlet-excited C$_{60}$ moiety but not electron transfer in toluene:

$$\text{4T-C}_{60} \xrightarrow[\text{in toluene}]{h\nu(<400\text{ nm})} {}^1\text{4T*-C}_{60} \xrightarrow{\text{energy transfer}} \text{4T-}{}^1\text{C}_{60}{}^* \quad (1)$$

Furthermore, no apparent acceleration of the decay rate of fluorescence from the C$_{60}$ moiety excludes photoinduced reactions from 4T-$^1$C$_{60}$* in toluene.

When 4T-C$_{60}$ was excited in more polar solvents, such as benzonitrile, the fluorescence band due to the C$_{60}$ moiety was quenched. The fluorescence decay profile around 710 nm in benzonitrile (Figure 3b) can be divided into two components; from the time-resolved fluorescence spectra, fast- and slow-decaying parts can be attributed to fluorescence from the C$_{60}$ moiety and the 4T moiety, respectively. Quenching of 4T-$^1$C$_{60}$*

**TABLE 1: Free-Energy Changes for Charge Separation ($-\Delta G_{CS}$), Fluorescence Lifetimes ($\tau_F$), Singlet Quenching Rate Constants ($k_q^S$), and Quantum Yields for Charge Separation ($\Phi_{CS}$) in a 4T-$C_{60}$ Dyad in Various Solvents**

| fullerene | solvent[a] | $\epsilon_{solv}$[b] | $-\Delta G_{CS}$/eV[c] | $\tau_F$/s | $k_q^S$/s$^{-1}$[d] | $\Phi_{CS}$[e] |
|---|---|---|---|---|---|---|
| 4T-$C_{60}$ | BN | 25.2 | 0.11 | $5.5 \times 10^{-11}$ | $1.7 \times 10^{10}$ | 0.96 |
| | ANS/BN | 14.8 | 0.08 | $7.8 \times 10^{-11}$ | $1.2 \times 10^{10}$ | 0.94 |
| | THF | 7.58 | −0.03 | $3.4 \times 10^{-11}$ | $2.8 \times 10^{10}$ | 0.97 |
| | ANS | 4.33 | −0.19 | $1.9 \times 10^{-10}$ | $4.5 \times 10^{9}$ | 0.85 |
| | ANS/Tol | 3.36 | −0.29 | $4.6 \times 10^{-10}$ | $1.4 \times 10^{9}$ | 0.65 |
| | Tol | 2.38 | −0.48 | $1.3 \times 10^{-9}$ | $<10^{8}$ | <0.1 |
| NMPC$_{60}$[f] | Bz | 2.28 | | $1.3 \times 10^{-9}$ | | |

[a] BN, benzonitrile; ANS/BN, anisole/benzonitrile (1:1) mixture; THF, tetrahydrofuran; ANS, anisole; ANS/Tol, anisole/toluene (1:1) mixture; Tol, toluene; Bz, benzene. [b] Data from ref 23. [c] $-\Delta G_{CR}^{II} = E_{ox} - E_{red} + \Delta G s$, $-\Delta G_{CS} = \Delta E_{0-0} - (-\Delta G_{CR})$, $\Delta G s = e^2/(4\pi\epsilon_0)[(1/(2R^+) + 1/(2R^-) - 1/R_{cc})(1/\epsilon_s) - (1/(2R^+) + 1/(2R^-))(1/\epsilon_r)]$ where $\Delta E_{0-0}$ is the energy of the 0−0 transition of $C_{60}$; $E_{ox}$ and $E_{red}$ are the first oxidation potential of the donor and the first reduction potential of the acceptor in benzonitrile, respectively. $R^+$ and $R^-$ are radii of 4T (7.5 Å) and $C_{60}$ (4.2 Å), respectively; $R_{cc}$ is the center-to-center distance between the two moieties (13.0 Å); and $\epsilon_s$ and $\epsilon_r$ are static dielectric constants of solvents used for the rate measurements and the redox-potential measurements. [d] $k_q^S = (\tau_F)^{-1} - (\tau_0)^{-1}$, where $\tau_0$ is the fluorescence lifetime of NMPC$_{60}$ in toluene. [e] $\Phi_{CS} = ((\tau_F)^{-1} - (\tau_0)^{-1})/((\tau_F)^{-1})$. [f] Data from ref 17.

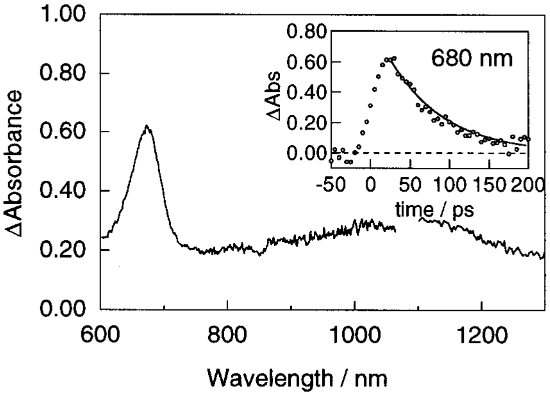

**Figure 4.** Picosecond transient absorption spectrum of 4T-$C_{60}$ in benzonitrile at 20 ps after 532-nm laser irradiation. Insert is absorption−time profile at 680 nm. Solid line shows fitted curve.

indicates photoinduced processes including charge separation in the dyad. The possibility of energy transfer to the 4T moiety can be excluded because of a higher singlet energy of 4T (2.70 eV) than of $C_{60}$ (1.74 eV). Actually, the fluorescence lifetime of 4T-$^1C_{60}$* ($\tau_F$) in nonpolar toluene was the same as that of NMPC$_{60}$ (1.3 ns)[17] within experimental error (Figure 3a). The fluorescence lifetime of 4T-$^1C_{60}$* became shorter with an increase of the solvent polarity, as listed in Table 1. The reaction rate constant ($k_q^S$) in each solvent was estimated from the relation $k_q^S = (\tau_F)^{-1} - (\tau_0)^{-1}$, where $\tau_0$ is the fluorescence lifetime of NMPC$_{60}$ in toluene, as summarized in Table 1.

**Picosecond Laser Flash Photolysis.** To obtain more detailed information on the photoinduced processes of 4T-$^1C_{60}$*, transient absorption spectra in the picosecond regime were observed. Figure 4 shows a transient absorption spectrum of 4T-$C_{60}$ in benzonitrile obtained with 532-nm laser light irradiation of the $C_{60}$ moiety. At 20 ps after the laser irradiation, sharp and broad transient absorption bands were observed at 680 and 1140 nm, respectively. Because of accordance with an absorption spectrum of the radical cation of 4T (4T$^{\bullet+}$),[14,18] both transient absorption bands can be attributed to the radical cation of the 4T moiety, indicating photoinduced charge separation in the 4T-$C_{60}$ dyad molecule (eq 2):

$$\text{4T-C}_{60} \xrightarrow{h\nu(532\text{ nm})} \text{4T-}^1\text{C}_{60}{}^* \xrightarrow{k_{CS}} \text{4T}^{\bullet+}\text{-C}_{60}{}^{\bullet-} \quad (2)$$

An absorption band due to the radical anion of $C_{60}$ moiety, which would be anticipated to appear around 1000 nm,[17] should be hidden by the intense absorption band of the 4T radical cation around 1140 nm, because an extinction coefficient of the absorption band of 4T$^{\bullet+}$ in this wavelength region is larger than that of $C_{60}{}^{\bullet-}$.[14] Similar charge separations were also observed in anisole/benzonitrile mixture, tetrahydrofuran, anisole, and anisole/toluene mixture solvents. Exciplex formation can be excluded because the absorption bands due to the 4T$^{\bullet+}$ moiety did not shift with solvent polarity.

The absorption−time profile at 680 nm (insert of Figure 4) can be analyzed by assuming the first-order rise and decay functions. Since the estimated rise rate was close to the value of the present instrumental resolution, the $k_q^S$ values from fluorescence were adopted as reaction rate constants for the present charge-separation reaction ($k_{CS}$). This treatment can be rationalized by the absence of an energy-transfer reaction from the $^1C_{60}$* to the 4T moiety upon 532 nm-laser irradiation. As mentioned in above section, the $k_{CS}$ value ($= k_q^S$) increased with increasing solvent polarity (Table 1). The quantum yield for the charge separation ($\Phi_{CS}$) can be calculated from the relation $\Phi_{CS} = k_{CS}/(k_{CS} + k_0) = ((\tau_F)^{-1} - (\tau_0)^{-1})/((\tau_F)^{-1})$, where $k_0$ is the fluorescence decay rate of NMPC$_{60}$. The $\Phi_{CS}$ values are also increased with an increase of solvent polarity, as summarized in Table 1. The estimated $\Phi_{CS}$ value is as high as 0.97 in tetrahydrofuran. The $\Phi_{CS}$ values close to unity indicate efficient charge separation in the dyad molecule with short donor−acceptor linkage in polar solvents. As for the dyad molecule including fullerene, the $\Phi_{CS}$ values close to unity have been reported for the zinc porphyrin−$C_{60}$ dyad and the carotene−$C_{60}$ dyad,[2−4] indicating a potential for application to light-harvesting systems or solar cells.[4c] Furthermore, the $\Phi_{CS}$ and $k_{CS}$ values of the present dyad molecule are similar in tetrahydrofuran, anisole/benzonitrile mixture, and benzonitrile. This finding indicates that charge separation in these solvents corresponds to those around the top region of the Marcus parabola. Free-energy changes for the charge separation ($\Delta G_{CS}$) were estimated as listed in Table 1 using the Born equation. The $k_{CS}$ values are plotted against the $\Delta G_{CS}$ values as shown in Figure 5. Since $k_{CS}$ values show maximum values with small $\Delta G_{CS}$ values, reorganization energy for the present dyad molecule is considered to be small, as proposed by Imahori et al. for the $C_{60}$−porphyrin dyad molecule.[4b]

As shown in the inserted figure of Figure 4, generated radical ions decreased after reaching a maximum at ca. 20 ps. The decay of the absorption bands of the radical ions can be attributed to the charge recombination in the dyad molecule. By applying the first-order decay function, the rate for the charge recombination ($k_{CR}^I$), in which suffix I refers to the first step of charge recombination, was estimated to be $1.5 \times 10^{10}$ s$^{-1}$. The $k_{CR}^I$ values estimated for the other reaction media are listed in Table 2 as well as the free-energy changes for the charge recombina-

**TABLE 2: Free-Energy Changes ($-\Delta G_{CR}^{I}$ and $-\Delta G_{CR}^{II}$) and Rate Constants ($k_{CR}^{I}$ and $k_{CR}^{II}$) for Charge Recombination, Quantum Yields for Triplet Formation ($\Phi_T$), and Triplet Decay Rate Constants ($k_T$) of 4T-$C_{60}$ in Various Solvents**

| fullerene | solvent[a] | $-\Delta G_{CR}^{I}$/eV[b] | $k_{CR}^{I}$/s$^{-1}$ | $-\Delta G_{CR}^{II}$/eV[c] | $k_{CR}^{II}$/s$^{-1}$ | $\Phi_T$ | $k_T$/s$^{-1}$ |
|---|---|---|---|---|---|---|---|
| 4T-$C_{60}$ | BN | 0.13 | $1.5 \times 10^{10}$ | 1.63 | $1.6 \times 10^{5}$ | [d] | [d] |
| | ANS/BN | 0.16 | $1.2 \times 10^{10}$ | 1.66 | $1.2 \times 10^{5}$ | [d] | [d] |
| | THF | 0.22 | $2.4 \times 10^{10}$ | 1.77 | [e] | [e] | [e] |
| | ANS | 0.43 | $4.2 \times 10^{9}$ | 1.93 | | $0.7 \pm 0.15$ | $3.9 \times 10^{4}$ |
| | ANS/Tol | 0.53 | $8.7 \times 10^{8}$ | 2.03 | | $1.0 \pm 0.15$ | $3.4 \times 10^{4}$ |
| | Tol | 0.72 | [f] | 2.22 | | $1.0 \pm 0.15$ | $3.2 \times 10^{4}$ |
| NMPC$_{60}$[g] | Bz | | | | | 0.95 | $4.1 \times 10^{4}$ |

[a] Abbreviations for solvents: see caption of Table 1. [b] $\Delta G_{CR}^{I} = \Delta G_{CR}^{II} - E_T$, where $E_T$ is the energy level of 4T-$^3C_{60}$*. [c] See caption of Table 1. [d] A transient absorption band due to 4T-$^3C_{60}$* was not observed. [e] Estimation was difficult due to overlap with $4T^{\bullet+}$-$C_{60}^{\bullet-}$. [f] Transient absorption bands due to $4T^{\bullet+}$-$C_{60}^{\bullet-}$ were not observed. [g] Data from ref 17.

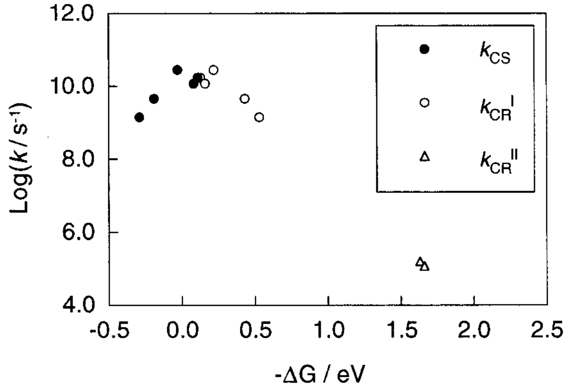

**Figure 5.** Relation between rate constants and free energy changes in various solvents. Filled circles, open circles, and triangles indicate $k_{CS}$, $k_{CR}^{I}$, and $k_{CR}^{II}$, respectively.

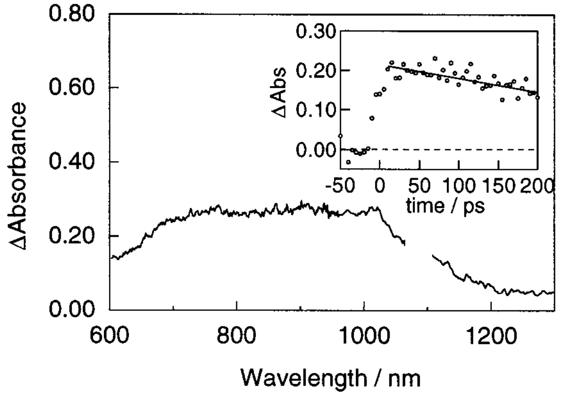

**Figure 6.** Picosecond transient absorption spectra of 4T-$C_{60}$ in toluene at 70 ps after 532-nm laser irradiation. Insert is absorption−time profile at 980 nm. Solid line shows fitted curve.

tion process ($\Delta G_{CR}^{I}$) for generating triplet excited $C_{60}$ (4T-$^3C_{60}$*), since the charge recombination of $4T^{\bullet+}$-$C_{60}^{\bullet-}$ generates 4T-$^3C_{60}$* predominantly, as mentioned in the next section. The $k_{CR}^{I}$ values increased with an increase in solvent polarity, that is, the dielectric constant ($\epsilon_{solv}$). Fast charge recombination for less negative $\Delta G_{CR}^{I}$ values indicates that the charge recombination process is in the Marcus inverted region (Figure 5).

As for 4T-$C_{60}$ in toluene, transient absorption bands due to charge separation were not observed (Figure 6). A broad absorption band around 900 nm can be attributed to 4T-$^1C_{60}$* from similarity with an $S_n \leftarrow S_1$ absorption band of $C_{60}$.[19] The absorption band decreased slowly, as indicated in the insert figure of Figure 6. The finding indicates that no charge separation takes place in nonpolar toluene because of an unstable charge-separated state relative to the 4T-$^1C_{60}$* state. The decay of 4T-$^1C_{60}$* can be attributed to the intersystem crossing to 4T-$^3C_{60}$*.

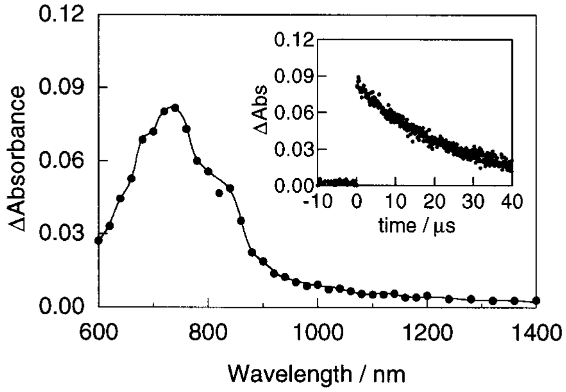

**Figure 7.** Nanosecond transient absorption spectrum of 4T-$C_{60}$ in anisole at 100 ns after 532-nm laser irradiation. Insert is absorption−time profile at 720 nm.

**Nanosecond Laser Flash Photolysis.** Figure 7 shows a transient absorption spectrum of 4T-$C_{60}$ in anisole after nanosecond laser excitation. Absorption bands with a peak at 700 nm can be attributed to 4T-$^3C_{60}$*.[17] Actually, the whole absorption band was quenched efficiently in the presence of oxygen, a triplet quencher. Similarly, 4T-$^3C_{60}$* formation was observed in the anisole/toluene mixture and in toluene, that is, moderately polar and nonpolar solvents. The generation of 4T-$^3C_{60}$* can be attributed to recombination of $4T^{\bullet+}$-$C_{60}^{\bullet-}$ as well as the intersystem crossing from 4T-$^1C_{60}$*. Since the quantum yield for the intersystem crossing process of NMPC$_{60}$ is reported to be 0.95,[17] quantum yields for 4T-$^3C_{60}$* formation by the intersystem crossing from 4T-$^1C_{60}$* are 0.14, 0.33, and 0.95 in anisole, anisole/toluene mixture, and toluene, respectively, from ($1 - \Phi_{CS}$) values. From the relative actinometry method using $^3C_{70}$* as an internal standard (T−T peak 980 nm, $\epsilon = 6500$ M$^{-1}$cm$^{-1}$, and $\Phi_{isc} = 0.9 \pm 0.15$)[20] and the reported extinction coefficient for triplet excited NMPC$_{60}$,[17] the quantum yields for 4T-$^3C_{60}$* formation ($\Phi_T$), which are the total of deactivation from 4T-$^1C_{60}$* and $4T^{\bullet+}$-$C_{60}^{\bullet-}$, were estimated to be 0.7, 1.0, and 1.0 in anisole, anisole/toluene mixture, and toluene, respectively. These quite large quantum yields indicate that $4T^{\bullet+}$-$C_{60}^{\bullet-}$ deactivates to generate 4T-$^3C_{60}$* predominantly in less polar solvents. That is, deactivation from 4T-$^1C_{60}$* and $4T^{\bullet+}$-$C_{60}^{\bullet-}$ to the ground state is a minor process in the present dyad molecule. Charge recombination processes, to give mainly the triplet excited states, are also reported for a fullerene−tris(2,2′-bipyridine)ruthenium dyad molecule by Maggini et al.[6b] and for a carotene−porphyrin fullerene triad molecule by Liddell et al.[21] Charge separation and recombination processes of the present dyad molecule in polar solvents are summarized in a schematic energy diagram (Figure 8a), in addition to energy transfer processes in a nonpolar solvent (Figure 8b).

In polar solvents, the formation of $^34T$*-$C_{60}$ by the deactivation from $4T^{\bullet+}$-$C_{60}^{\bullet-}$ can be excluded from the energetic

(a) in polar solvent

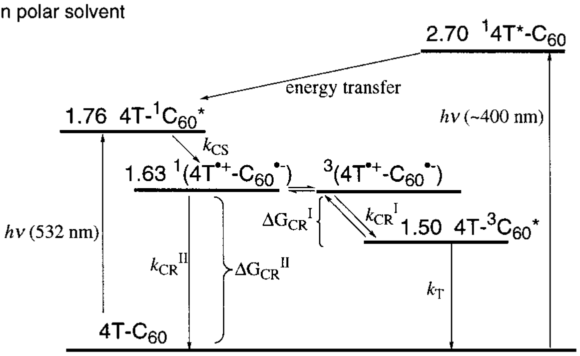

(b) in non-polar solvent

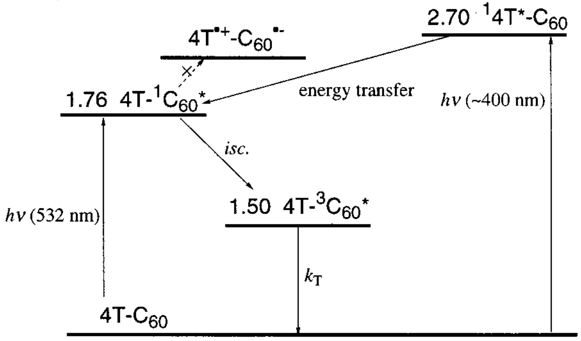

**Figure 8.** Schematic energy diagrams for charge separation and charge recombination processes in the 4T-$C_{60}$ dyad (a) in polar (benzonitrile) and (b) nonpolar (toluene) solvents. Numbers indicate energy levels in eV units relative to the ground state.

consideration: Triplet energy of 4T is as high as 1.9 eV,[14] which is larger than $4T^{\bullet+}$-$C_{60}^{\bullet-}$ and 4T-$^{1}C_{60}^{*}$ (Figure 8a). Actually, absorption bands due to the $^{3}4T^{*}$ moiety, which are reported to appear at 550 and 620 nm,[18] were not observed in the nanosecond transient absorption spectrum.

The decay rate constants of 4T-$^{3}C_{60}^{*}$ ($k_T$) were estimated from the transient absorption band at 700 nm to be 3−4 × $10^4$ $s^{-1}$ in anisole, anisole/toluene mixture, and toluene, which are quite close to values of the triplet decay rate constant of NMPC$_{60}$ in benzene (4.1 × $10^4$ $s^{-1}$).[17] The finding indicates that generated 4T-$^{3}C_{60}^{*}$ deactivates to the ground state by intersystem crossing without further reaction processes in these less polar solvents and in the nonpolar solvent. The estimated decay rate constants are summarized in Table 2.

In the case of 4T-$C_{60}$ in benzonitrile, a transient absorption spectrum observed by the nanosecond laser flash photolysis shows peaks at 1140 and 680 nm, which undoubtedly indicate existence of $4T^{\bullet+}$-$C_{60}^{\bullet-}$ in the microsecond time region (Figure 9). An absorption band due to the radical anion of the $C_{60}$ moiety may be hidden by the absorption band of the radical cation of the 4T moiety, as in the case of the picosecond laser flash photolysis. The shoulder around 840 nm is assigned to 4T-$^{3}C_{60}^{*}$ from comparison with the transient absorption spectra of 4T-$^{3}C_{60}^{*}$ (Figure 7) and $4T^{\bullet+}$-$C_{60}^{\bullet-}$ (Figure 4). From the absorption−time profile at 1140 nm, the decay rate constant of $4T^{\bullet+}$-$C_{60}^{\bullet-}$ ($k_{CR}^{II}$), in which suffix II refers to the second charge recombination step, was estimated to be 1.6 × $10^5$ $s^{-1}$, which corresponds to 6.3 $\mu$s of lifetime. In the tetrahydrofuran and anisole/benzonitrile solvents the absorption bands due to $4T^{\bullet+}$-$C_{60}^{\bullet-}$ were also observed overlapping with 4T-$^{3}C_{60}^{*}$ in the microsecond time region (Figure 10). The $k_{CR}^{II}$ value in anisole/benzonitrile mixture was estimated to be 1.2 × $10^5$ $s^{-1}$, whereas the $k_{CR}^{II}$ value in tetrahydrofuran was difficult to estimate due to spectral overlap with 4T-$^{3}C_{60}^{*}$. The estimated lifetimes for the second charge separation step are quite longer than other reported donor−acceptor dyad molecules, for which the radical ions show lifetimes in the subnanosecond region.[2−6]

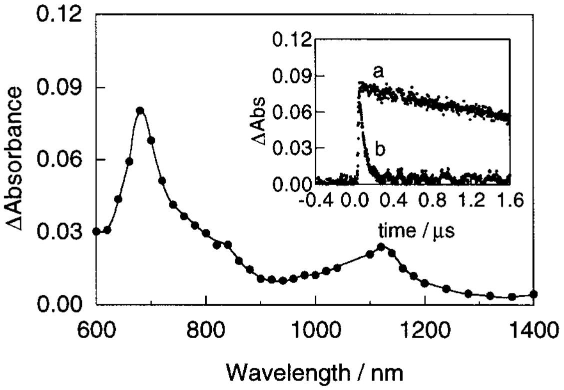

**Figure 9.** Nanosecond transient absorption spectrum of 4T-$C_{60}$ in benzonitrile at 100 ns after 532-nm laser irradiation. Insert is absorption−time profile at 680 nm in the (a) absence and (b) presence of oxygen.

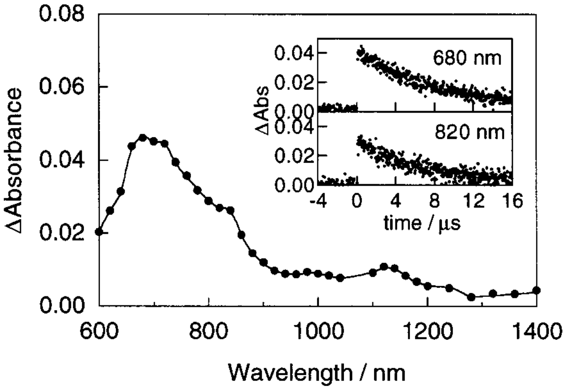

**Figure 10.** Nanosecond transient absorption spectrum of 4T-$C_{60}$ in anisole/benzonitrile mixture at 100 ns after 532-nm laser irradiation. Insert is absorption−time profile at 680 and 820 nm.

It is worth mentioning that the absorption bands due to $4T^{\bullet+}$-$C_{60}^{\bullet-}$, as well as that of 4T-$^{3}C_{60}^{*}$, were quenched in the presence of oxygen, as indicated in the inserted figure of Figure 9. It has been reported that the radical anion of $C_{60}$ in a triad molecule was not quenched by oxygen, indicating that electron transfer does not occur to $O_2$ from the $C_{60}^{\bullet-}$ moiety after complete charge transfer.[22] Therefore, such oxygen-sensitive radical ions in the present dyad molecule may be attributed to radical ion pair generation from triplet excited state; a triplet exciplex, that is, $^{3}(4T^{\delta+}$-$C_{60}^{\delta-})^{*}$; or an equilibrium between the radical ion pair ($4T^{\bullet+}$-$C_{60}^{\bullet-}$) and 4T-$^{3}C_{60}^{*}$. In the present case, the last mechanism seems to be plausible, because the absorption band due to 4T-$^{3}C_{60}^{*}$ was observed in polar solvents as well as those of $4T^{\bullet+}$-$C_{60}^{\bullet-}$ (Figures 9 and 10). A typical case is shown in Figure 10; in the transient absorption spectrum, 820- and 720-nm bands are due to 4T-$^{3}C_{60}^{*}$, whereas 1140- and 680-nm bands are due to $4T^{\bullet+}$-$C_{60}^{\bullet-}$. Furthermore, this mechanism will be rationalized by the fact that the decay rate of $4T^{\bullet+}$-$C_{60}^{\bullet-}$ is the same as that of 4T-$^{3}C_{60}^{*}$ in anisole/benzonitrile mixture (insert of Figure 10). The energy difference between $4T^{\bullet+}$-$C_{60}^{\bullet-}$ and 4T-$^{3}C_{60}^{*}$ becomes large in less polar solvents, in which 4T-$^{3}C_{60}^{*}$ becomes dominant in the equilibrium, as observed in the nanosecond transient absorption spectrum (Figure 10).

For radical ion pairs, state $^{3}(4T^{\bullet+}$-$C_{60}^{\bullet-})$ may be in equilibrium with $^{1}(4T^{\bullet+}$-$C_{60}^{\bullet-})$ as illustrated in Figure 8a. The deactivation of these radical ion pairs to the ground state is considered to proceed via $^{1}(4T^{\bullet+}$-$C_{60}^{\bullet-})$, of which the rate should be faster than $k_T$ due to the same spin multiplicity. In Table 2, free-energy changes for the deactivation from $^1(4T^{\bullet+}\text{-}C_{60}{}^{\bullet-})$ to the ground state ($\Delta G_{CR}{}^{II}$) in various solvents are also listed. Smaller $k_{CR}{}^{II}$ values than $k_{CR}{}^{I}$ seem to be reasonable, since $\Delta G_{CR}{}^{II}$ values are more negative than $\Delta G_{CR}{}^{I}$ and the charge recombination processes are in the inverted region (Figure 5).

## Conclusion

The present 4T-$C_{60}$ dyad produced a high yield of a charge-separated state upon laser irradiation of the $C_{60}$ moiety in polar solvents, even though the small free-energy change was expected for this charge separation. This finding accords with small reorganization energies of dyad molecules, including $C_{60}$. The first charge-recombination step in the dyad was found to generate triplet excited $C_{60}$ at a yield close to unity. Furthermore, in polar solvents in which the energy level of the charge-separated state locates at close to the triplet excited state, the lifetime of the second charge-separated state was on the order of microseconds. The unprecedentedly long lifetime of the charge-separated state in the dyad molecule was considered to result from an equilibrium between the charge-separated state and the triplet excited state. Such a long lifetime of the charge-separated state seems to be useful to further applications such as novel sensitized reactions.

**Acknowledgment.** The present work is partly supported by a Grant-in Aid on Scientific Research in Priority Area (B) on “Laser Chemistry of a Single Nanometer Organic Particle” (No. 10207202) and No. 11740380 from the Ministry of Education, Science, Sports, and Culture, Japan.

## References and Notes

(1) Williams, R. M.; Zwier, J. M.; Verhoeven, J. W. *J. Am. Chem. Soc.* **1995**, *117*, 4093.

(2) (a) Imahori, H.; Cardoso, S.; Tatman, D.; Lin, S.; Noss, L.; Seely, G. R.; Sereno, L.; Silber, C.; Moore, T. A.; Moore, A. L.; Gust, D. *Photochem. Photobiol.* **1995**, *62*, 1009. (b) Gust, D.; Moore, T. A.; Moore, A. L. *Res. Chem. Intermed.* **1997**, *23*, 621.

(3) Kuciauskas, D.; Lin, S.; Seely, G. R.; Moore, A. L.; Moore, T. A.; Gust. D.; Drovetskaya, T.; Reed, C. A.; Boyd, P. D. W. *J. Phys. Chem.* **1996**, *100*, 15926.

(4) (a) Imahori, H.; Hagiwara, K.; Aoki, M.; Akiyama, T.; Taniguchi, S.; Okada, T.; Shirakawa, M.; Sakata, Y. *J. Am. Chem. Soc.* **1996**, *118*, 11771. (b) Imahori, H.; Hagiwara, K.; Akiyama, T.; Aoki, M.; Taniguchi, S. S.; Okada, T.; Shirakawa, M.; Sakata, Y. *Chem. Phys. Lett.* **1996**, *263*, 545. (c) Imahori, H.; Ozawa, S.; Uchida, K.; Takahashi, M.; Azuma, T.; Ajavakom, A.; Akiyama, T.; Hasegawa, M.; Taniguchi, S.; Okada, T.; Sakata, Y. *Bull. Chem. Soc. Jpn.* **1999**, *72*, 485.

(5) Guldi, D. M.; Garscia, G. T.; Mattay, J. *J. Phys. Chem. A* **1998**, *102*, 9679.

(6) (a) Sariciftci, N. S.; Wudl, F.; Heeger, A. J.; Maggini, M.; Scorrano, G.; Prato, M.; Bourassa, J.; Ford, P. C. *Chem. Phys. Lett.* **1995**, *247*, 510. (b) Maggini, M.; Guldi, D. M.; Mondini, S.; Scorrano, G.; Paolucci, F.; Ceroni, P.; Roffia, S. *Chem.—Eur. J.* **1998**, *4*, 1992. (c) Polese, A.; Mondini, S.; Bianco, A.; Toniolo, C.; Scorrano, G.; Guldi, D. M.; Maggini, M. *J. Am. Chem. Soc.* **1999**, *121*, 3446. (d) Guldi, D. M.; Maggini, M.; Scorrano, G.; Prato, M. *J. Am. Chem. Soc.* **1997**, *119*, 975.

(7) (a) Senssion, R. J.; Phillips, C. M.; Szarka, A. Z.; Romanow, W. J.; McGhie, A. R.; McCauley, J. P.; Smith, A. B.; Hochstrasser, R. M. *J. Phys. Chem.* **1991**, *95*, 6075. (b) Dimitrijevic, N. M.; Kamat, P. V. *J. Phys. Chem.* **1992**, *96*, 4811. (c) Palit, D. K.; Sapre, A. V.; Mittal, J. P.; Rao, C. N. R. *Chem. Phys. Lett.* **1992**, *195*, 1.

(8) (a) Arbogast, J. W.; Foote, C. S. *J. Am. Chem. Soc.* **1991**, *113*, 8886. (b) Arbogast, J. W.; Foote, C. S.; Kao, M. *J. Am. Chem. Soc.* **1992**, *114*, 2277. (c) Nonell, S.; Arbogast, J. W.; Foote, C. S. *J. Phys. Chem.* **1992**, *96*, 4169. (d) Zhang, X.; Foote, C. S. *J. Am. Chem. Soc.* **1995**, *117*, 4271. (e) Zhang, X.; Fan, A.; Foote, C. S. *J. Org. Chem.* **1996**, *61*, 5465. (f) Bernstein, R.; Prat, F.; Foote, C. S. *J. Am. Chem. Soc.* **1999**, *121*, 464.

(9) (a) Guldi, D. M.; Hungerbuhler, H.; Asmus, K.-D. *J. Phys. Chem.* **1995**, *99*, 9380. (b) Guldi, D. M.; Hungerbuhler, H.; Asmus, K.-D. *J. Phys. Chem.* **1995**, *99*, 13487. (c) Guldi, D. M.; Hungerbuhler, H.; Asmus, K.-D. *J. Phys. Chem. A* **1997**, *101*, 1783. (d) Guldi, D. M. *J. Phys. Chem. A* **1997**, *101*, 3895. (e) Thomas, K. G.; Biju, V.; George, M. V.; Guldi, D. M.; Kamat, P. V. *J. Phys. Chem. A* **1998**, *102*, 5341. (f) Guldi, D. M.; Torres-Garcia, G.; Mattay, J. *J. Phys. Chem. A* **1998**, *102*, 9679. (g) Guldi, D. M.; Hungerbuhler, H.; Asmus, K. D. *J. Phys. Chem. B.* **1999**, *103*, 1444. (h) Polese, A.; Mondini, S.; Bianco, A.; Toniolo, C.; Scorrano, G.; Guldi, D. M.; Maggini, M. *J. Am. Chem. Soc.* **1999**, *121*, 3446.

(10) (a) Biczok, L.; Linschitz, H.; Walter, R. I. *Chem. Phys. Lett.* **1992**, *195*, 339. (b) Sterein, C. A.; van Willigen, H.; Bizók. L.; Gupta, N.; Linschitz, H. *J. Phys. Chem.* **1996**, *100*, 8920. (c) Biczok, L.; Gupta, N.; Linschitz, H. *J. Am. Chem. Soc.* **1997**, *119*, 12601. (d) Gupta, N.; Linschitz, H.; Biczok, L. *Full. Sci. Technol.* **1997**, *5*, 343.

(11) (a) Mikami, K.; Matsumoto, S.; Tonoi, T.; Suenobu, T.; Ishida, A.; Fukuzumi, S. *Synlett* **1997**, 85. (b) Fukuzumi, S.; Suenobu, T.; Kawamura, S.; Ishida, A.; Mikami, K. *Chem. Commun.* **1997**, 291. (c) Fukuzumi, S. *Res. Chem. Intermed.* **1997**, *23*, 519. (d) Fukuzumi, S.; Suenobu, T.; Patz, M.; Hirasaka, T.; Itoh, S.; Fujitsuka, M.; Ito, O. *J. Am. Chem. Soc.* **1998**, *120*, 8060. (e) Fukuzumi, S.; Suenobu, T.; Fujitsuka, M.; Ito, O.; Tonoi, T.; Matsumoto, S.; Mikami, K. *J. Organomet. Chem.* **1999**, *574*, 32.

(12) (a) Sasaki, Y.; Fujitsuka, M.; Watanabe, A.; Ito, O. *J. Chem. Soc., Faraday Trans.* **1997**, *93*, 4275. (b) Nojiri, T.; Alam, M. M.; Konami, H.; Watanabe, A.; Ito, O. *J. Phys. Chem. A* **1997**, *101*, 7943. (c) Nojiri, T.; Watanabe, A.; Ito, O. *J. Phys. Chem. A* **1998**, *102*, 5215. (d) Alam, M. M.; Sato, M.; Watanabe, A.; Akasaka, T.; Ito, O. *J. Phys. Chem. A* **1998**, *102*, 7447. (e) Luo, C. P.; Fujitsuka, M.; Huang, C. H.; Ito, O. *J. Phys. Chem. A* **1998**, *102*, 8716. (f) El-Kemary, M.; Fujitsuka, M.; Ito, O. *J. Phys. Chem. A* **1999**, *103*, 1329. (g) Akasaka, T.; Suzuki, T.; Maeda, Y.; Ara, M.; Wakahara, T.; Kobayashi, K.; Nagase, S.; Kako, M.; Nakadaira, Y.; Fujitsuka, M.; Ito, O. *J. Org. Chem.* **1999**, *64*, 566.

(13) Janssen, R. A. J.; Sariciftci, N. S.; Heeger, A. J. *J. Phys. Chem.* **1994**, *100*, 8641.

(14) Matsumoto, K.; Fujitsuka, M.; Sato, T.; Onodera, S.; Ito, O., submitted for publication.

(15) (a) Sariciftci, N. S.; Smilowitz, L.; Heeger, A. J.; Wudl, F. *Science* **1992**, *258*, 1474. (b) Sariciftci, N. S.; Heeger, A. J. *Int. J. Mod. Phys. B* **1994**, *8*, 237.

(16) Yamashiro, T.; Aso, Y.; Otsubo, T.; Tang, H.; Harima, T.; Yamashita, K. *Chem. Lett.* **1999**, 443.

(17) Luo, C. P.; Fujitsuka, M.; Watanabe, A.; Ito, O.; Gan, L.; Huang, Y.; Huang, C. H. *J. Chem. Soc., Faraday Trans.* **1998**, *84*, 527.

(18) Wintgens, V.; Valat, P.; Garnier, F. *J. Phys. Chem.* **1994**, *98*, 228.

(19) Ebbesen, T. W.; Tanigaki, K.; Kuroshima, S. *Chem. Phys. Lett.* **1991**, *181*, 501.

(20) (a) Arbogast, J. W.; Foote, C. S. *J. Am. Chem. Soc.* **1991**, *113*, 8886. (b) Guldi, D. M.; Hungerbuhler, H.; Janata, E.; Asmus, K.-D. *J. Phys. Chem.* **1993**, *97*, 11258. (c) Fraelich, M. R.; Weisman, R. B. *J. Phys. Chem.* **1993**, *97*, 11145.

(21) Liddell, P. A.; Kuciauskas, D.; Sumida, J. P.; Nash, B.; Nguyen, D.; Moore, A. L.; Moore, T. A.; Gust, D. *J. Am. Chem. Soc.* **1997**, *119*, 1400.

(22) Fujitsuka, M.; Ito, O.; Imahori, H.; Yamada, K.; Yamada, H.; Sakata, Y. *Chem. Lett.* **1999**, 721.

(23) Murov, S. L.; Carmichael, I.; Hug, G. L. *Handbook of Photochemistry* 2nd ed.; Marcel Dekker: New York, 1993.